NUMERICAL DOMAIN WALL TYPE SOLUTIONS IN ϕ^4 THEORY

J. KARKOWSKI

Institute of Theoretical Physics, Jagellonian University
30-059 Kraków, Reymonta 4, Poland

AND

Z. ŚWIERCZYŃSKI

Institute of Physics, Pedagogical University
Podchorążych 2, 30-084 Kraków, Poland

(Received July 27, 1996)

The well known domain wall type solutions are nowadays of great physical interest in classical field theory. These solutions can mostly be found only approximatelly. Recently the Hilbert–Chapman–Enskog method was succesfully applied to obtain this type solutions in ϕ^4 theory. The goal of the present paper is to verify these perturbative results by numerical computations.

PACS numbers: 02.60.Cb

1. Introduction

During the last few years domain walls, strings and vortices have been of great physical interest in classical and quantum field theory. These are the solutions of highly non-linear partial differential equations with the energy concentrated in a small region of the whole space-time. They play an important role in cosmology, condensed matter and elementary particles theory. Usually the exact form of these solutions can not be obtained as the appropriate equations are too difficult to integrate. There are many approximate methods which can help to solve these equations but they usually do not provide the quantitative estimation of errors. Thus they should be compared with the numerical solutions obtained with help of the well tested algorithms. Numerical methods can also verify many assumptions which

must be made in perturbative calculations. In the present paper we consider the domain wall type solutions in ϕ^4 theory. We compare our numerical results with the approximate solutions obtained in [1]. These approximate solutions were found with help of the so-called Hilbert–Chapman–Enskog method [7]. It is the singular perturbative scheme [8] as the small perturbation parameter appears in the term with the highest order derivatives. Thus from the mathematical point of view the problem is very subtle and its numerical verification is especially valuable. Let us stress that the paper [1] is the part of the larger program [2–5] devoted to studying different approximate methods in classical field theory. Many technical problems have been examined in this program so far and that is the second reason why we extend it on numerical analysis.

2. Approximate solutions

In this section we shortly describe the approximated domain wall type solutions in ϕ^4 theory proposed in [1]. The lagrangian density and the corresponding field equation have the form

$$L = -\frac{1}{2}\eta_{\mu\nu}\partial^\mu\Phi\partial^\nu\Phi - \frac{\lambda}{2}\left(\Phi^2 - \frac{M^2}{4\lambda}\right)^2, \tag{1}$$

$$\partial_\mu\partial^\mu\Phi - 2\lambda\left(\Phi^2 - \frac{M^2}{4\lambda}\right)\Phi = 0. \tag{2}$$

Here $(\eta_{\mu\nu}) = \mathrm{diag}(-1,1,1,1)$ is the metric tensor and λ , M are some positive constants. There exist two classical vacuum solutions in this model, namely $\Phi = \pm M/2\sqrt{\lambda}$. A domain wall type solution smoothly interpolates between these two vacua. It is convenient to introduce in Minkowski space the special coordinate system (u^0, u^1, u^2, s) co-moving with the domain wall [1, 6]. The three coordinates u^0, u^1, u^2 describe the world volume of the membrane attached to the domain wall and $\xi = 2s/M$ is the distance from this three-dimensional hypersurface (for details see [1]). Thus

$$x^\mu = Y^\mu(u) + \xi n^\mu(u), \tag{3}$$

where the functions $Y^\mu(u)$ describe the above mentioned hypersuface and $n^\mu(u)$ is the normalised four-vector orthogonal to it. In these new coordinates the equation of motion takes the form

$$\frac{2}{M^2}\frac{1}{\sqrt{-G}}\frac{\partial}{\partial u^a}\left(\sqrt{-G}G^{ab}\frac{\partial\phi}{\partial u^b}\right) + \frac{1}{2}\frac{\partial^2\phi}{\partial s^2} + \frac{1}{2h}\frac{\partial h}{\partial s}\frac{\partial\phi}{\partial s} - (\phi^2 - 1)\phi = 0, \tag{4}$$

where

$$\Phi(x^\mu) = \frac{M}{2\sqrt{\lambda}}\phi(u^a, s), \tag{5}$$

$$G_{ab} = N_{ac}g^{cd}N_{db}, N_{ac} = g_{ac} - \xi K_{ac}, \tag{6}$$

$$\sqrt{-G} = \sqrt{-g}h, g = \det[g_{ab}], G = \det[G_{ab}]. \tag{7}$$

The induced metric g_{ab} and the external curvature K_{ac} are defined by

$$K_{ab} = n_\mu \partial_a \partial_b Y^\mu, g_{ab} = \partial_a Y^\mu \partial_b Y_\mu. \tag{8}$$

The Hilbert–Chapman–Enskog method has been applied in [1] to obtain the perturbative solution of the equation (4). According to this method the following form is assumed for the approximate solution of the equation (4)

$$\phi = \phi^{(0)} + \frac{1}{M}\phi^{(1)} + \frac{1}{M^2}\phi^{(2)} + \dots . \tag{9}$$

In the present paper this approximation is verified numerically to give very precise results. However in general the problem is a little bit more complicated as the equation (4) involves the small perturbation parameter in the term with the highest order derivative. Usually in such case one can expect the solution to involve some extra non-analytic terms which of course are absent in the formula (9). This problem is discussed mainly from the physical point of view in [1]. The non-analitic terms can really exist in the general solution but they are only radiative corrections to the base domain-wall configuration. These terms can be completely removed from the solution by the appropriate choice of the initial conditions. This is the case we are especially interested in as we would like to extract the pure domain-wall type solution without radiation. In practice it is very difficult to find the desired initial conditions. However even if the radiative corrections are present they quite rapidly decrease with time as the whole solution tends to the stable domain-wall type configuration. Thus these possible extra terms can practically be neglected. This is the reason why the Hilbert-Enskog-Chapman method could be safely applied in [1]. We will return to this problem in our conclusions. Assuming that for $u^0 = 0$ the surface $\phi = 0$ coincides with the membrane $s = 0$ the result looks as follows

$$\begin{aligned}\phi = \tanh s + \frac{1}{M}\frac{C}{\cosh^2 s} \\ - \frac{1}{M^2}\left[C^2\left(\frac{6f_1(s)}{\cosh^2 s} + \frac{\phi_2^{(2)}(s)}{\cosh^6 s}\right) + 4K_a^b K_b^a\left(\frac{f_1(s)}{\cosh^2 s} + f_3(s)\phi_2^{(2)}(s)\right)\right] \\ + \dots ,\end{aligned} \tag{10}$$

where

$$\phi_2^{(2)} = \frac{1}{8}\sinh(2s) + \frac{3}{8}\tanh s + \frac{3}{8}\frac{s}{\cosh^2 s}, \tag{11}$$

$$f_1(s) = \int_0^s dx \frac{\sinh x}{\cosh^5 x}\phi_2^{(2)}(x), \tag{12}$$

$$f_2(s) = \int_0^s dx \frac{x}{\cosh^2 x}\phi_2^{(2)}(x), \tag{13}$$

$$f_3(s) = -\int_0^s dx \frac{x}{\cosh^4 x} \tag{14}$$

and the function $C(u^a)$ satisfies the equation

$$\Box^{(3)}C + \left(\frac{\pi^4}{4} - 1\right) K_a^b K_b^a C + \frac{9}{35}C^3 = \left(\frac{\pi^2}{6} - 1\right) K_c^a K_a^b K_b^c, \tag{15}$$

with initial conditions

$$C(u^0 = 0) = \frac{\partial C}{\partial u^0}(u^0 = 0) = 0. \tag{16}$$

Here the symbol $\Box^{(3)}$ denotes the three-dimensional d'Alembertian on the membrane surface. The function $C(u^a)$ determines the position of the surface where the field ϕ vanishes. This position is given by the formula

$$s = -\frac{C}{M} + O(M^{-3}). \tag{17}$$

3. Numerical results

We have examined in detail two special cases of the general result (10), namely the cylindrical and the spherical domain walls. In the cylindrical case the function $C(u^a)$ and the invariant $K_c^a K_a^b K_b^c$ vanish. The other invariant $K_b^a K_a^b$ takes the simple form

$$K_a^b K_b^a = 2\frac{r_0^2}{r^4}, \tag{18}$$

where

$$r(u^0) = r_0 \cos \frac{u^0}{r_0} \tag{19}$$

and r_0 is the initial position of the domain wall. Let us stress that in this case the position of the surface where the field ϕ vanishes coincides with the membrane attached to the domain wall, at least up to the second order in $1/M$. The equation of motion (4) for the cylindrical domain wall reads as

$$\frac{\partial}{\partial u^0}\left(\frac{r+\xi\frac{r_0}{r}}{\frac{r}{r_0}-\frac{\xi}{r}}\frac{\partial\phi}{\partial u^0}\right)+\left(r+\xi\frac{r}{r_0}\right)\left(\frac{r}{r_0}-\frac{\xi}{r}\right) \times\left(\frac{\partial^2\phi}{\partial\xi^2}-2\frac{\xi r_0^2}{r^4-\xi^2 r_0^2}\frac{\partial\phi}{\partial\xi}-\frac{M^2}{2}\left(\phi^2-1\right)\phi\right)=0. \tag{20}$$

The spherical case is a little bit more complicated because both invariants $K^a_b K^b_a$ and $K^a_c K^b_a K^c_b$ are different from zero

$$K^b_a K^a_b = 6\frac{r_0^4}{r^6}, \tag{21}$$

$$K^a_c K^b_a K^c_b = 6\frac{r_0^6}{r^9}, \tag{22}$$

where

$$r(u^0) = r_0 \mathrm{cn}\left(\sqrt{2}\frac{u^0}{r_0}, \frac{1}{2}\right). \tag{23}$$

As a consequence the function $C(u^a)$ does not vanish and should be obtained numerically. Thus in this case the distance between the above mentioned surfaces is different from zero. The appropriate equation of motion for the spherical domain wall takes the form

$$\frac{\partial}{\partial u^0}\left(\frac{r+\xi\frac{r_0^2}{r^2}}{\frac{r^2}{r_0^2}-2\frac{\xi}{r}}\frac{\partial\phi}{\partial u^0}\right)+\left(r+\xi\frac{r_0^2}{r^2}\right)\left(\frac{r^2}{r_0^2}-2\frac{\xi}{r}\right) \times\left(\frac{\partial^2\phi}{\partial\xi^2}-6\frac{\xi r_0^4}{r^6-\xi r^3 {r_0}^2-2\xi^2 r_0^4}\frac{\partial\phi}{\partial\xi}-\frac{M^2}{2}\left(\phi^2-1\right)\phi\right)=0. \tag{24}$$

We have solved the equations (20) and (24) numerically for $-0.5 \leq \xi \leq 0.5$ and $0 \leq u^0 \leq 1$ with the initial data $\phi|_{u^0=0}, \partial\phi/\partial u^0|_{u^0=0}$ computed from formula (10) with $K^a_b K^b_a$ given by (18) or (21) respectively. Let us note that the maximal value of u^0 can not be too big because of possible singularities

in the coordinate system [2]. We have introduced a grid of 8000 points and the partial derivatives with respect to ξ have been replaced with

$$\frac{\partial\phi}{\partial\xi} \approx \frac{\phi_{n+1} - \phi_{n-1}}{2\Delta\xi}, \frac{\partial\phi^2}{\partial^2\xi} \approx \frac{\phi_{n+1} - 2\phi_n + \phi_{n-1}}{(\Delta\xi)^2}. \tag{25}$$

The system of ordinary differential equations obtained this way has been integrated by the Runge–Kutta method [9]. The numerical computations in both cases *e.g.* cylindrical and spherical have been performed for $r_0 = 2.5$ and three different values of the parameter $M = 10, 20, 40$. We have compared the numerical functions $\phi_{\mathrm{num}}(u^0 = 1.0)$ and $\partial\phi_{\mathrm{num}}/\partial u^0(u^0 = 1.0)$ with their approximate counterparts $\phi_{\mathrm{ap}}(u^0 = 1.0)$ and $\partial\phi_{\mathrm{ap}}/\partial u^0(u^0 = 1.0)$ obtained from formula (10). The motion of the surface $\phi = 0$ has been also computed and compared with the approximate result (17). Figures 1–4 show the differences $\Delta\phi = \phi_{\mathrm{num}} - \phi_{\mathrm{ap}}$ and $\Delta\phi_{u^0} = \partial\phi_{\mathrm{num}}/\partial u^0 - \partial\phi_{\mathrm{ap}}/\partial u^0$ in the case of the cylindrical domain wall. We do not present the functions ϕ_{num} themselves because the interesting higher order corrections are very small compared to the u^0 independent term $\phi^{(0)} = \tanh(s)$. Instead the difference $\phi_{\mathrm{num}} - \tanh(s)$ is presented in Fig. 5 for $M = 20$. The corresponding derivative $\partial\phi/\partial u^0$ is shown in Fig. 6. The motion of the core $\phi_{\mathrm{num}} = 0$ is plotted in figures 13–15. Let us recall that in this case $C \equiv 0$ and the surface $\phi_{\mathrm{ap}} = 0$ coincides with the membrane $s = 0$. The differences $\Delta\phi$ and $\Delta\phi_{u^0}$ in the spherical case are presented in figures 7–10. Figures 11 and 12 are the spherical counterparts of 5 and 6. The motion of the core $\phi_{\mathrm{num}} = 0$ and the correspondig results computed from the formula (17) for $\phi_{\mathrm{ap}} = 0$ are plotted in figures 16–18.

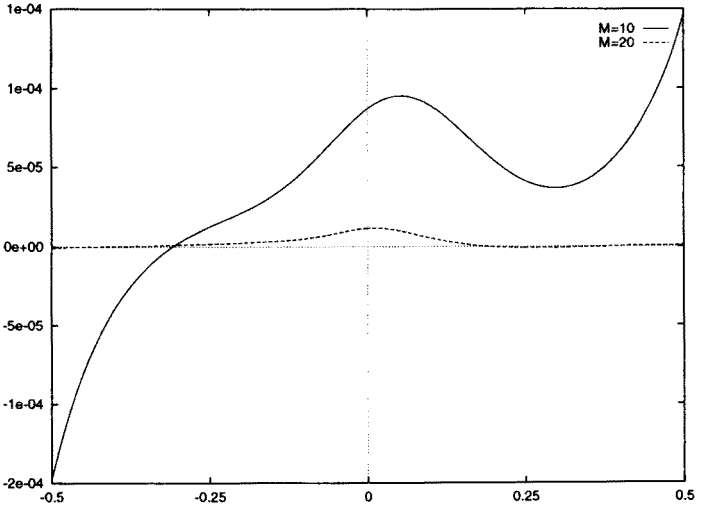

Fig. 1. The differences $\Delta\phi(u^0 = 1.0)$ for the cylindrical domain wall, $M = 10$ and $M = 20$.

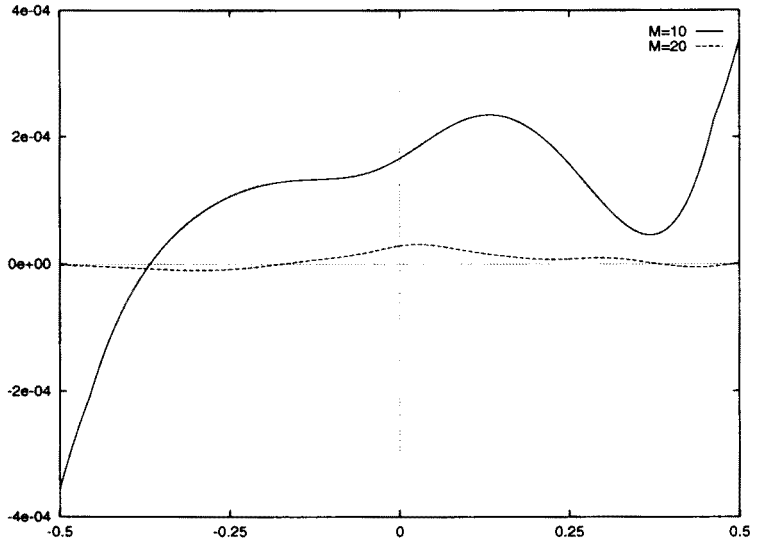

Fig. 2. The differences $\Delta\phi_{u^0}(u^0 = 1.0)$ for the cylindrical domain wall, $M = 10$ and $M = 20$.

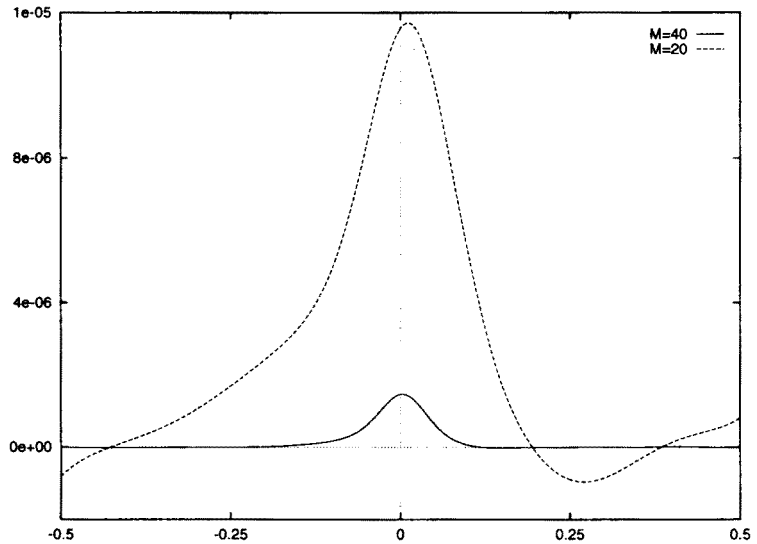

Fig. 3. The differences $\Delta\phi(u^0 = 1.0)$ for the cylindrical domain wall, $M = 20$ and $M = 40$.

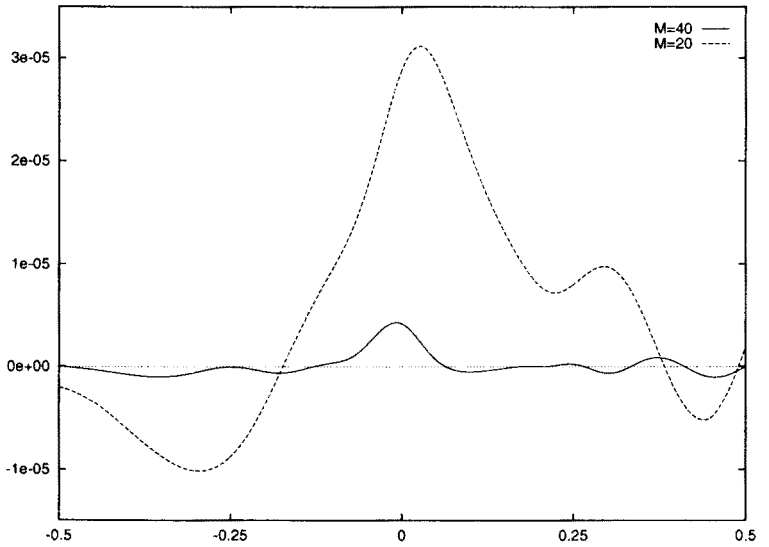

Fig. 4. The differences $\Delta\phi_{u^0}(u^0 = 1.0)$ for the cylindrical domain wall, $M = 20$ and $M = 40$.

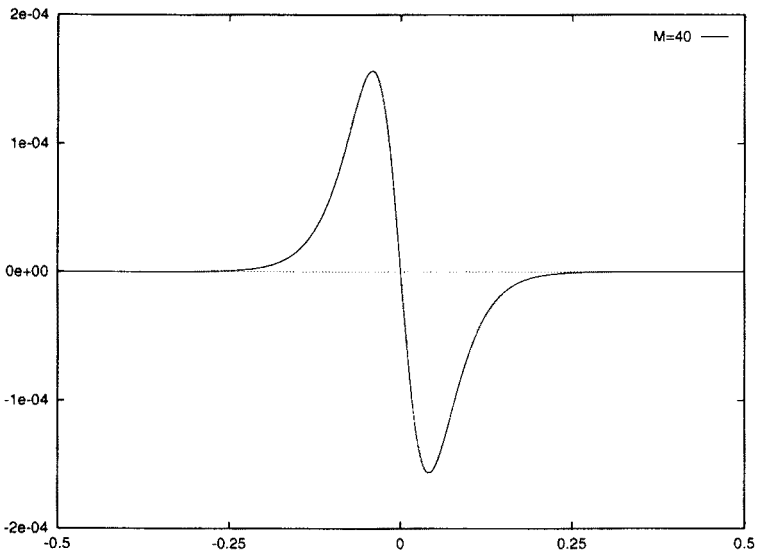

Fig. 5. The difference $\phi_{\text{num}}(u^0 = 1.0) - \tanh(s)$ for the cylindrical domain wall, $M = 40$.

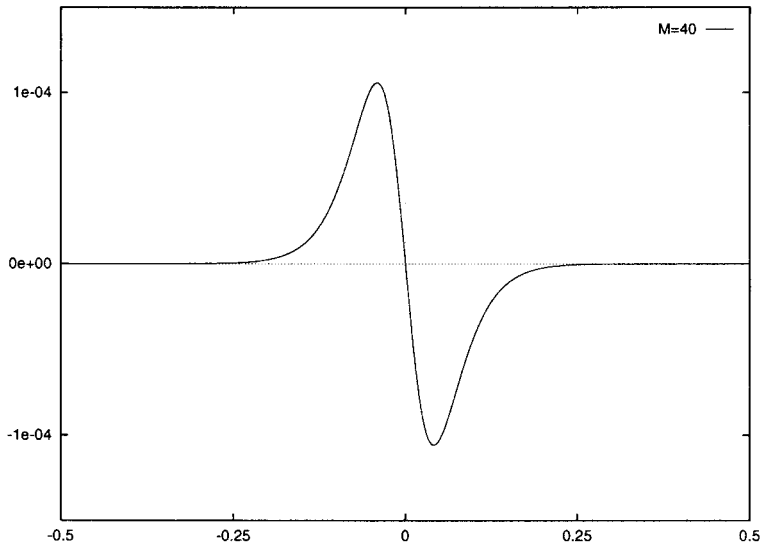

Fig. 6. The derivative $\partial\phi/\partial u^0(u^0 = 1.0)$ for the cylindrical domain wall $M = 40$.

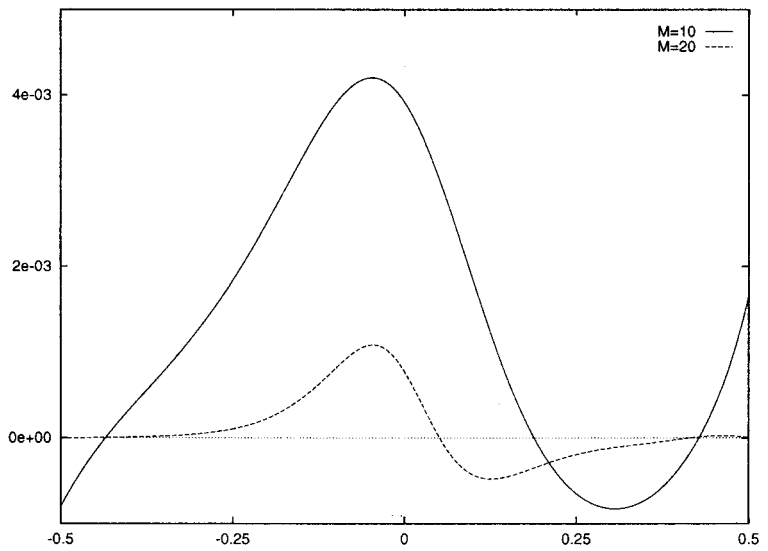

Fig. 7. The differences $\Delta\phi(u^0 = 1.0)$ for the spherical domain wall, $M = 10$ and $M = 20$.

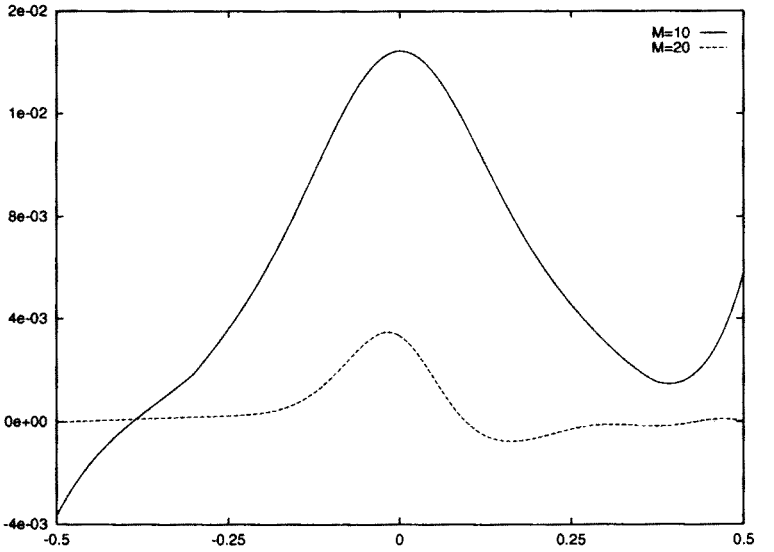

Fig. 8. The differences $\Delta\phi_{u^0}(u^0 = 1.0)$ for the spherical domain wall, $M = 10$ and $M = 20$.

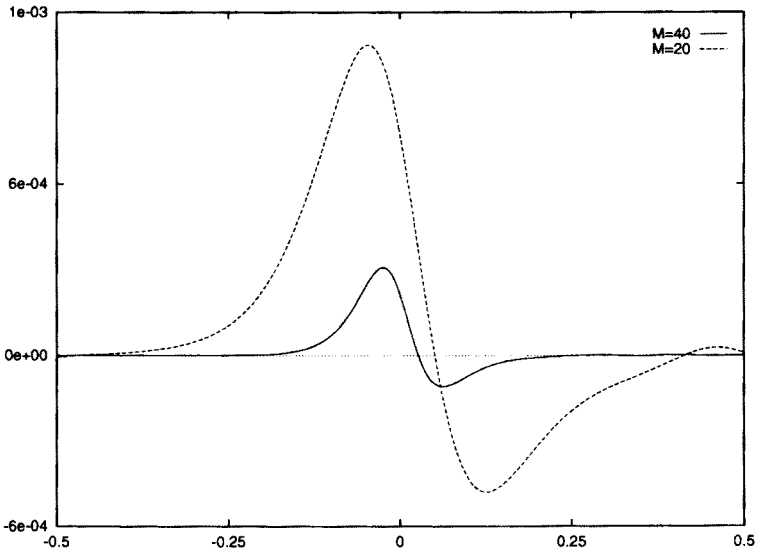

Fig. 9. The differences $\Delta\phi(u^0 = 1.0)$ for the spherical domain wall, $M = 20$ and $M = 40$.

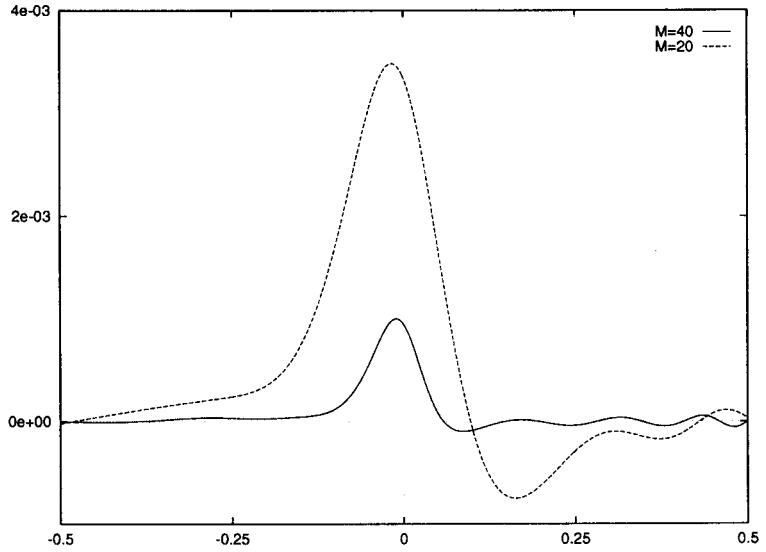

Fig. 10. The differences $\Delta\phi_{u^0}(u^0 = 1.0)$ for the spherical domain wall, $M = 20$ and $M = 40$.

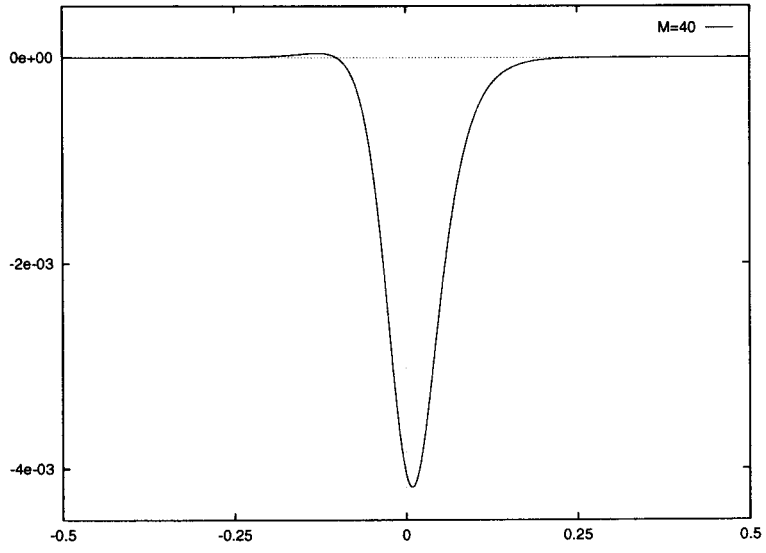

Fig. 11. The difference $\phi_{\text{num}}(u^0 = 1.0) - \tanh(s)$ for the spherical domain wall, $M = 40$.

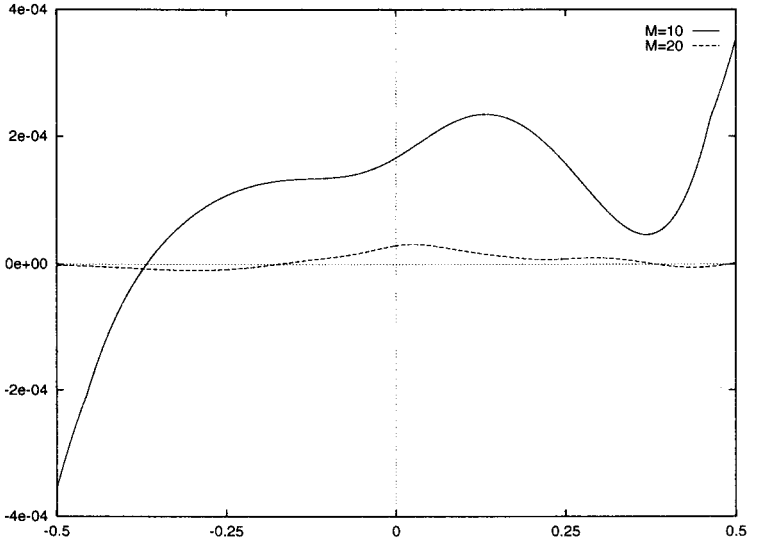

Fig. 12. The derivative $\partial\phi/\partial u^0(u^0 = 1.0)$ for the spherical domain wall $M = 40$.

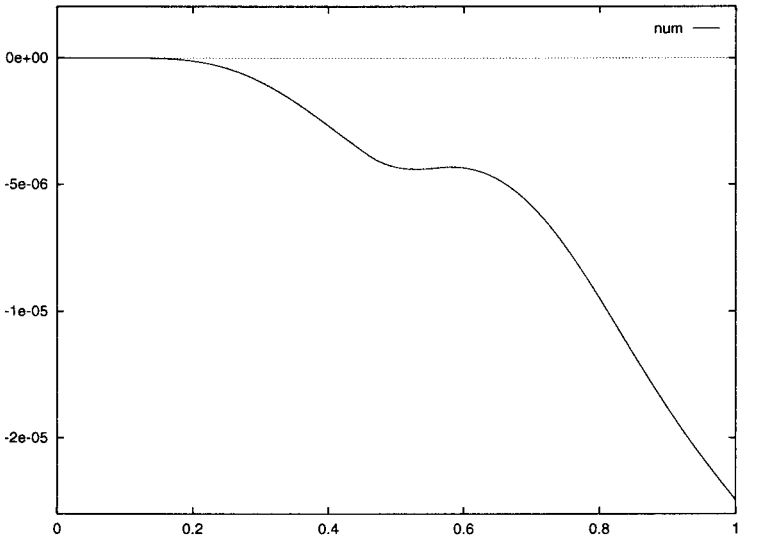

Fig. 13. The motion of the surface $\phi_{\text{num}} = 0$ for the cylindrical domain wall, M=10.

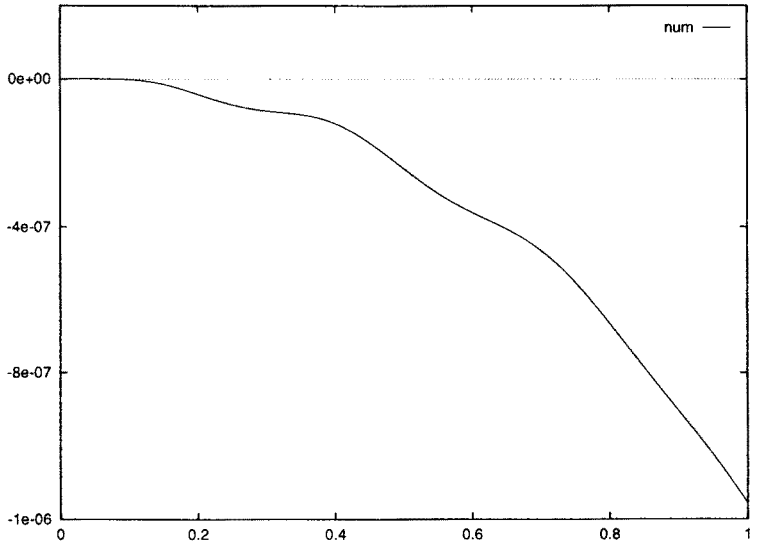

Fig. 14. The motion of the surface $\phi_{\text{num}} = 0$ for the cylindrical domain wall, M=20.

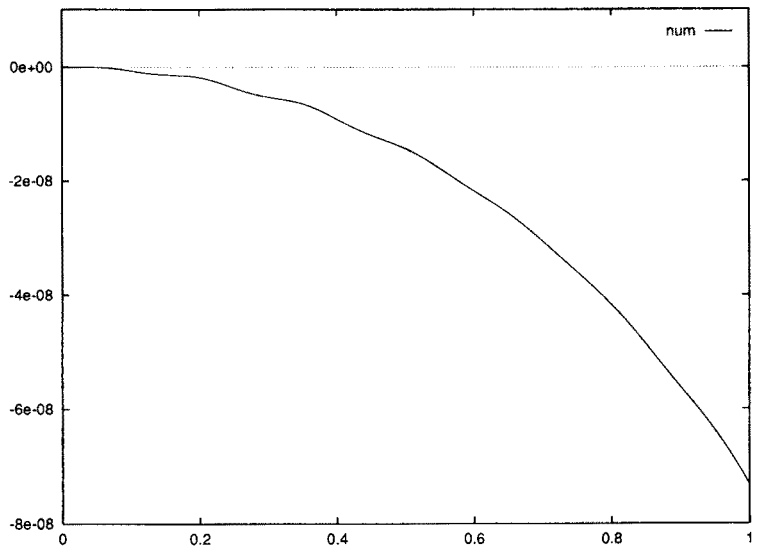

Fig. 15. Fig. 15. The motion of the surface $\phi_{\text{num}} = 0$ for the cylindrical domain wall M=40.

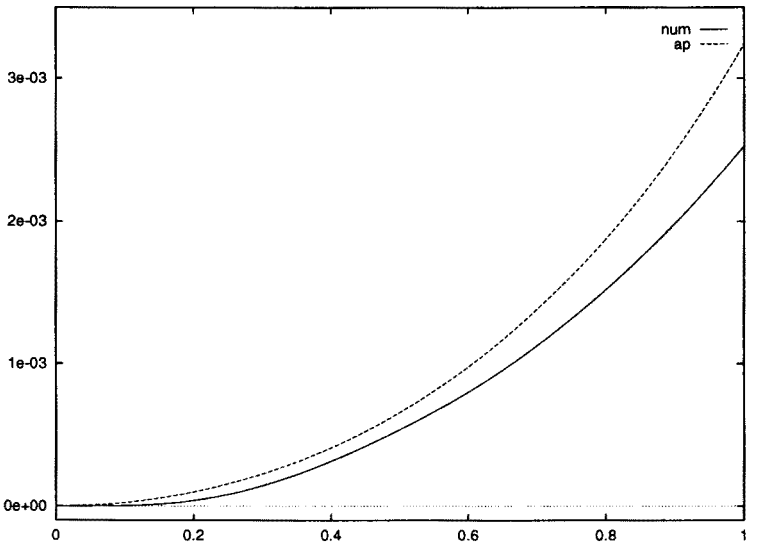

Fig. 16. The motion of the surfaces $\phi_{\text{num}} = 0$ and $\phi_{\text{ap}} = 0$ for the spherical domain wall, M=10.

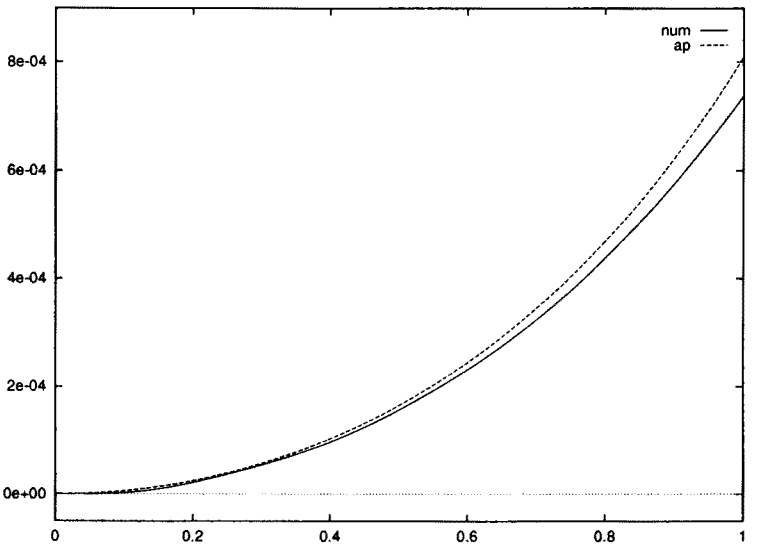

Fig. 17. The motion of the surfaces $\phi_{\text{num}} = 0$ and $\phi_{\text{ap}} = 0$ for the spherical domain wall, M=20.

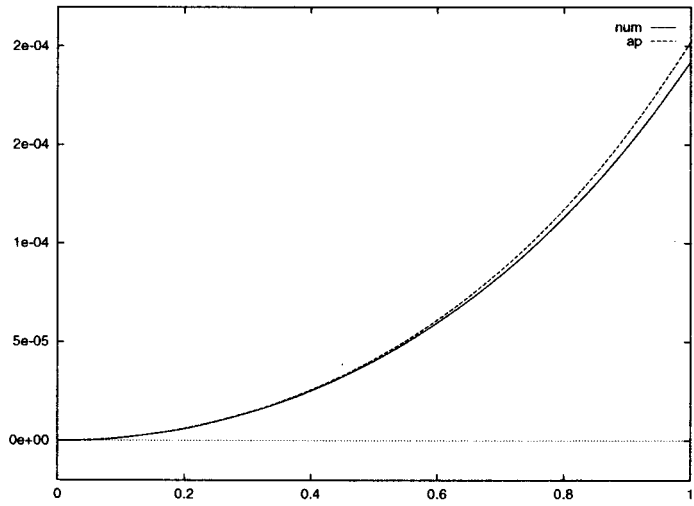

Fig. 18. The motion of the surfaces $\phi_{\text{num}} = 0$ and $\phi_{\text{ap}} = 0$ for the spherical domain wall, M=40.

4. Conclusions

The aim of our paper was to verify the approximate solutions proposed in [1] by the numerical computations. Our investigations prove that the coincidence of the numerical results and the approximate ones is quite good. The existing differences could be affected by radiative corrections absent in the perturbative scheme. In numerical calculations these corrections can not be completely removed. However our results show that these possible terms are small and can be neglected in our considerations as the perturbative solution is only known up to the second order term in $1/M$. It would be interesting to compare these radiative corrections with the higher order terms of the perturbative scheme. This is the argument for further studies of these important questions. As it should be expected the differences $\phi_{\text{num}} - \phi_{\text{ap}}$ and $\partial\phi_{\text{num}}/\partial u^0 - \partial\phi_{\text{ap}}/\partial u^0$ decrease rather rapidly when the models with thinner walls (bigger M) are considered. Let us also stress that the numerical and the approximated motion of the domain wall almost coincide for our biggest value of the parameter M. Thus the approximation proposed in [1] seems to be an efficient tool to examine important details of some peculiar solutions in classical field theory like domain walls or vortices. In general our paper proves that the progress in the practical dealing with non-linear partial differential equations can be achieved when one combines different clever approaches such as the Hilbert–Enskog–Chapman perturbative method and the suitable choice of the coordinate system.

REFERENCES

[1] H. Arodź, *Nucl. Phys.* **B450**, 174 (1995).
[2] H. Arodź, A. L. Larsen, *Phys. Rev.* **D49**, 4154 (1994).
[3] H. Arodź, *Phys. Rev* **D52**, 1082 (1995).
[4] H. Arodź, *Nucl. Phys.* **B450**, 189 (1995).
[5] H. Arodź, L. Hadasz, preprint TPJU - 8/95, June 1995 (hep-th/9506021).
[6] R. Gregory, *Phys. Lett.* **B206**, 199 (1988); R. Gregory, D. Haws, D. Garfinkle, *Phys. Rev.* **D42**, 343 (1990); V. Silveira, M.D. Maia, *Phys. Lett.* **A174**, 280 (1993); A.L. Larsen, *Phys. Lett.* **A181**, 369 (1993).
[7] N.G. van Kampen, *Stochastic Processes in Physics and Chemistry.* North-Holand Publ. Comp., Amsterdam 1987. Chapt. 8, §7.
[8] S.A. Lomov, *Vvedenie v Obscuju Teoriju Singularnych Vozmuscenij.* Nauka, Moskva 1981, in Russian.
[9] W.H. Press, S.A. Teukolsky, W.T. Vetterling, B.P. Flannery, *Numerical Recipes in Fortran: The Art of Scientific Computing.* Cambridge University Press, New York 1992.